Combined Topological and Landau Order from Strong Correlations in Chern Bands

Stefanos Kourtis and Maria Daghofer
Institute for Theoretical Solid State Physics, IFW Dresden, 01171 Dresden, Germany
(Received 3 June 2013; revised manuscript received 2 October 2014; published 21 November 2014)

We present a class of states with both topological and conventional Landau order that arise out of strongly interacting spinless fermions in fractionally filled and topologically nontrivial bands with Chern number $C = \pm 1$. These quantum states show the features of fractional Chern insulators, such as fractional Hall conductivity and interchange of ground-state levels upon insertion of a magnetic flux. In addition, they exhibit charge order and a related additional trivial ground-state degeneracy. Band mixing and geometric frustration of the charge pattern place these lattice states markedly beyond a single-band description.

DOI: 10.1103/PhysRevLett.113.216404 PACS numbers: 71.27.+a, 03.65.Vf, 71.45.Lr, 73.43.−f

The fractional quantum Hall (FQH) effect is a paradigmatic example for a correlation-driven state with topological order [1], and the proposal [2–4] that the concept might be extended from Landau levels arising due to a magnetic field to topologically nontrivial bands on a lattice has thus raised considerable interest. The role of the magnetic field is then played by the band's Berry curvature and Coulomb repulsions are expected to stabilize analogs to FQH states. The fact that fractionally filled and topologically nontrivial bands with nonzero Chern number C can indeed host corresponding states, dubbed fractional Chern insulators (FCI), has since been well established numerically [2,5–8] for various models. Analytical considerations have established connections to FQH states by proposing wave functions [9,10] and pseudopotentials [11], as well as by noting the close mathematical relation between density operators in partially filled Chern bands and those of partially filled Landau levels [12–15]. As paths to realizing topologically nontrivial and nearly dispersionless bands, cold quantum gases [16,17], oxide interfaces [18] and layered oxides with an orbital degree of freedom [7,8], strained graphene [19], and organometallic systems [20] have been proposed. A review of this rapidly evolving field can be found in Ref. [21].

Apart from the intrinsic interest in such an effect, one motivation for the search of FCIs is their energy and thus temperature scale: because it is given by the scale of the interaction, it is expected to be considerably higher than the sub-Kelvin range of the FQH effect, especially for oxide-based proposals [7,8,18]. As one would, moreover, not need strong magnetic fields, both realization of such states and their potential application to qubits [22] then appear more feasible. It has been established that FCI states can survive the influence of several aspects that make bands on lattices different from perfectly flat Landau levels with uniform Berry curvature, e.g., finite dispersion [8,23], a moderate staggered chemical potential [2], disorder [24,25], or competition with a charge-density wave (CDW) [25].

Since the FQH effect can be discussed in tight-binding models instead of Landau levels [26,27], particularly intriguing features of FCI states are those that go beyond their FQH counterpart. FCIs with higher Chern numbers were discussed [23,28,29], which may be non-Abelian and thus suitable for quantum computation. It has also been noted that FCIs do not share the particle-hole symmetry of partially filled Landau levels [25,30]. All these extensions can, however, be understood by focusing exclusively on the fractionally filled Chern band. FCI states considered thus far are weakly interacting, in the sense that the interactions stabilizing them are too weak to mix in the other band(s) with different Chern numbers. Those can even be projected out of the Hamiltonian, which keeps the band topology intact but obscures the impact of other aspects, such as lattice geometry, again reflecting the similarity to Landau levels with their weak lattice potential.

In this Letter, we go beyond the limit of "weak" interactions into a regime where Chern bands with $C = +1$ and $C = -1$ mix. We find states that show the features of both a CDW (revealed by the charge structure factor) and a FCI (fractional Hall conductivity and spectral flow). The states are related to the "pinball liquid" of the triangular lattice [31] that combines charge-ordered with metallic [32,33] or superconducting [34] electrons. In the latter case, the system combines charge order with off-diagonal long-range order. Simultaneous existence of two such different order parameters has been extensively investigated, especially in its bosonic counterpart [35–38], the supersolid [39]. The present case, however, differs fundamentally from supersolids or superconducting pinball liquids, as the second type of order in addition to charge order is *topological*, i.e., nonlocal and without an order parameter. We thus arrive at an exotic state of matter that is characterized by both Landau-type and topological order and is understood in terms of both band topology and lattice geometry.

This novel class of states can be intuitively understood as being composed of particles that play two roles simultaneously. Most of them form the CDW occupying $1/3$ of the triangular lattice sites; see Fig. 1(b). As has been discussed in the context of the pinball liquid [31–33,40], additional

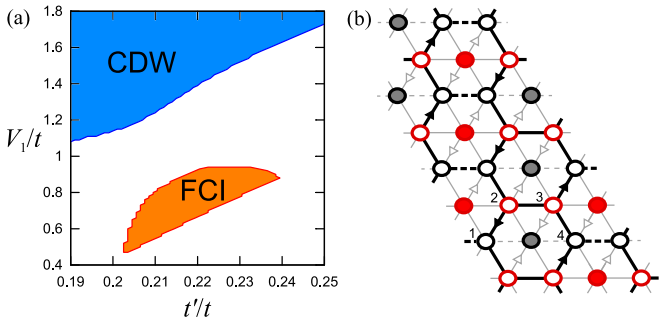

FIG. 1 (color online). CDW and FCI on the triangular lattice at $\nu = 2/3$ corresponding to $\bar{n} = 1/3$. (a) Phase diagram of model Eqs. (1a)–(1e) for a 3×3 unit-cell (6×3 lattice-site) system with six fermions and $V_2 = V_3 = 0$. (b) The $4 \times 4 - 1 = 15$ unit-cell (30 lattice-site) cluster used in this Letter: the unit cell (black or red circles) and the charge-order pattern (filled circles) arising in the CDW and the hoppings. Solid, dashed, and arrowed black lines represent complex hoppings with phases of 0, π, and $\pm\pi/2$, respectively. Gray lines denote hoppings deactivated by the CDW. Third nearest-neighbor hoppings are not shown.

particles can then move on the remaining sites, up to a total density of $\bar{n} = 2/3$ (two fermions per three lattice sites). One can view the remaining sites as an effective honeycomb-lattice model, which here has a four-site unit cell [see Fig. 1(b)] and is described by topologically nontrivial hoppings. Residual as well as longer-range Coulomb interactions will be shown here to induce a FCI out of the pinball liquid's metal, the topological pinball liquid (TPL).

Here, we discuss spinless fermions on a triangular lattice. The topologically nontrivial kinetic energy can be expressed in momentum space as

$$\mathcal{H}^0 = \sum_{\mathbf{k},\mu,\nu} c^\dagger_{\mathbf{k},\mu} H^0_{\mu,\nu}(\mathbf{k}) c_{\mathbf{k},\nu}, \tag{1a}$$

where the indices μ, ν refer to a two-site unit cell and $c^\dagger_{\mathbf{k},\mu}$ ($c_{\mathbf{k},\mu}$) are fermion creation (annihilation) operators. The momentum dependence is contained in the 2×2 matrix $H^0(\mathbf{k})$ expressed in terms of the vector of isospin Pauli matrices $\boldsymbol{\tau}$ and the unity matrix $\hat{I}$ as

$$H^0(\mathbf{k}) = \mathbf{g}(\mathbf{k}) \cdot \boldsymbol{\tau} + g_0(\mathbf{k}) \hat{I}, \tag{1b}$$

with

$$g_i(\mathbf{k}) = 2t \cos(\mathbf{k} \cdot \mathbf{a}_i), \qquad i = 1, 2, 3, \tag{1c}$$

and

$$g_0(\mathbf{k}) = 2t' \sum_{i=1}^{3} \cos(2\mathbf{k} \cdot \mathbf{a}_i). \tag{1d}$$

The unit cell and the phases of the hoppings can be seen in Fig. 1(b). $\mathbf{a}_1 = (1/2, -\sqrt{3}/2)^T$, $\mathbf{a}_2 = (1/2, \sqrt{3}/2)^T$, and $\mathbf{a}_3 = -(\mathbf{a}_1 + \mathbf{a}_2)$ are the triangular-lattice unit vectors. The nearest-neighbor (NN) and third nearest-neighbor hopping matrix elements are t and t', the latter is tuned to change the dispersion of the Chern band [25], with flattest bands arising for $t'/t \approx 0.2$. We keep $t'/t = 0.2$ unless mentioned otherwise, but we have verified that the main results remain valid for other values. The interaction

$$\mathcal{H}^1 = V_1 \sum_{\langle i,j \rangle} \hat{n}_i \hat{n}_j + V_2 \sum_{\langle\langle i,j \rangle\rangle} \hat{n}_i \hat{n}_j + V_3 \sum_{\langle\langle\langle i,j \rangle\rangle\rangle} \hat{n}_i \hat{n}_j \tag{1e}$$

is a repulsion of strength V_1 between NN sites, denoted by $\langle i, j \rangle$ and longer-range repulsion V_2 and V_3 between second and third neighbors, respectively. Here, we present results for $V_2 = V_3$, but have verified that unequal values do not qualitatively change the results unless very strong V_2 destabilizes the V_1-driven CDW. Operator $\hat{n}_i$ measures particle density at site i. While the model was originally introduced to describe topologically nontrivial phases in Kondo-lattice [41] and t_{2g} [8,25] systems—hence, the signs and phases in Eq. (1)—we use it here to study the more generic question of FCI states in the limit of strong interactions. We treat the model Eqs. (1a)–(1e) with Lanczos exact diagonalization on small clusters with periodic boundaries directly in real space, without projection onto the single-particle bands—both bands with Chern numbers $C = \pm 1$ are kept. We use clusters with 3×6 and 30 sites, which corresponds to 9 (15) unit cells, complemented by larger clusters in the limit of large V_1.

The model of Eq. (1) has been shown to yield FCI states at several filling fractions [8,25]. As the proposed TPL states we will be discussing below have both charge order and topological order, let us first briefly review these two phases and their signatures. For a filling of $\bar{n} = 1/3$ and small to moderate V_1, the electrons occupy $\nu = 2/3$ of the lower band and a corresponding FCI arises. CDW fluctuations destroy it at larger V_1; see the phase diagram Fig. 1(a) and Ref. [25]. A schematic picture of the CDW is given in Fig. 1(b).

Appropriate ground-state properties are necessary to determine the precise nature of the various phases. Charge order shows up in the charge-structure factor

$$N(\mathbf{k}) = \left| \sum_i e^{i\mathbf{k}\mathbf{r}_i} (\hat{n}_i - \bar{n}) |n\rangle \right|^2, \tag{2}$$

where $|n\rangle$ is a vector of the ground-state manifold and $\mathbf{r}_i$ denotes the location of site i. The CDW with $\bar{n} = 1/3$ induces sharp peaks at momenta $\mathbf{k} = \pm\mathbf{K}$, where $\mathbf{K} = (2\pi/3, 0)$, that grow with interaction strength V_1. In the FCI, their weight should remain comparable to that of other momenta [25].

FCI states, on the other hand, are identified by a fractional Hall conductivity σ_H, which is obtained by integrating the many-body Berry curvature in the $\boldsymbol{\varphi} = (\varphi_{\mathbf{a}_2}, \varphi_{\mathbf{a}_3})$ plane

of magnetic fluxes through the handles of the torus, where the fluxes are introduced as phase factors in the hoppings along $\mathbf{a}_2$ and $\mathbf{a}_3$, respectively. It is evaluated with the Kubo formula [25,42,43]:

$$\sigma_H = \frac{N_c}{\pi q}\sum_{n=1}^{q}\iint_0^{2\pi} d\varphi_{\mathbf{a}_2} d\varphi_{\mathbf{a}_3}\, \Im \sum_{n'\neq n} \frac{\langle n|\frac{\partial H}{\partial \varphi_{\mathbf{a}_3}}|n'\rangle\langle n'|\frac{\partial H}{\partial \varphi_{\mathbf{a}_2}}|n\rangle}{(\epsilon_n - \epsilon_{n'})^2}, \tag{3}$$

where N_c is the number of unit cells and $|n'\rangle$ are higher-energy eigenstates with eigenenergies $\epsilon_{n'}$. ϵ_n are the energies of the ground states. All values of σ_H are given in units of e^2/h. As this approach does not involve projections onto the lower (flat) band, it remains valid for arbitrary interactions and band mixing. In the FCI regime, we find a very precisely quantized $\sigma_H = 2/3$. For the 3×6-sites cluster, the ground states have the same momentum and the lowest-energy state contributes 2, while the other two states do not conduct, giving the expected average.

In both a CDW with $\bar{n} = 1/3$ and a FCI with $\nu = 2/3$, we expect a gapped ground-state manifold of three nearly degenerate states that are separated from the remaining spectrum by a gap. If their momenta are different, the FCI ground states are expected to exhibit spectral flow upon insertion of one flux quantum through one of the handles of the torus [44,45]. The closing of the gap for any value of the fluxes determines the phase boundaries in Fig. 1(a).

Using all eigenvalue and ground-state properties discussed, we trace the approximate phase diagram of the Hamiltonian given by Eq. (1) in Fig. 1(a), setting $V_2 = V_3 = 0$. Comparison to earlier results [25] for a lattice that is not commensurate with the CDW and hence suppresses it reveals substantial finite-size effects, but the presence and approximate location of both phases are consistent: The stability of the FCI depends both on V_1 and on the hopping t'; it is most stable for $t'/t \gtrsim 0.2$. At $\bar{n} = 1/3$, the CDW can always be induced by increasing V_1, and there is no coexistence of FCI and CDW phases.

Having recognized the main features of the FCI, the CDW, and their competition at $\bar{n} = 1/3$, we now turn to a phase having the defining features of both. Figure 2 gives the eigenvalue spectrum for fillings $\bar{n} = 12/30, 13/30$ and shows a 15-fold degenerate ground state as well as spectral flow. For the first case, the degeneracy expected for a straightforward FCI with $\nu = 12/15 = 4/5$ would be 5, which we did not observe for any interaction strength, instead of 15. In the second case, the degeneracy is consistent with a $\nu = 13/15$ FCI; however, levels return to their initial configuration already after insertion of only five flux quanta, which is unexpected. Moreover, additional interaction-generated dispersion tends to destabilize FCIs at such high fillings [15,30]. Closer inspection shows that the 15 low-energy states can be separated into three groups of five states each, where each group shows the spectral flow

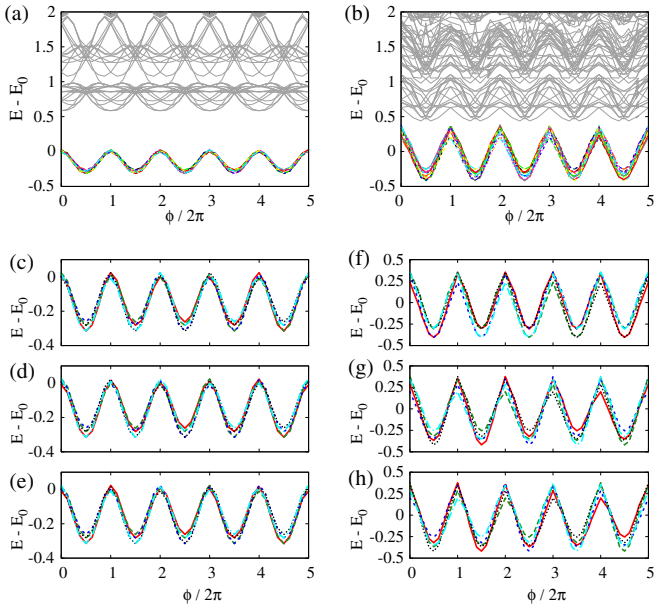

FIG. 2 (color online). Spectral flow upon flux insertion for the model of Eqs. (1a) and (1e) for a 15 unit-cell system at (a) $\nu = 12/15$ and (b) $\nu = 13/15$. In panels (c)–(e) [(f)–(h)], the 15 low-energy states of (a) [(b)] are divided into three groups of five; each group shows spectral flow consistent with a denominator-5 FCI. Fluxes are inserted as additional phases in the hoppings, totaling to φ for a loop around the cluster along direction $\mathbf{a}_3$. Parameters are $t'/t = 0.2$, $V_1/t = 10$, and $V_2 = V_3 = 2t$.

expected for a denominator-five state; see Figs. 2(c)–2(e) and 2(f)–2(h).

The Hall conductivity establishes this similarity to $\nu = 2/5$ ($\nu = 3/5$) states rather than 4/5 (13/15), as it is precisely quantized to $\sigma_H = 0.4$ ($\sigma_H = 0.6$) for each of the ground states. As in some FCI states, e.g., $\nu = 2/3$, the sum of contributions to the Hall conductivity does not add up to the Chern number of the noninteracting band. However, the present states are considerably more exotic as $\sigma_H = m/n$ at $\nu = p/q$, with $n \neq q$. The Hall conductivity is thus not given by the usual heuristic $\sigma_H = \nu \times C$. Similar to earlier observations for the FQH effect in the presence of an external potential [46], this is a strong indication that the "topological" degeneracy differs from the number of ground states and here is in both cases $n = 5$ rather than $q = 15$.

The remaining "trivial" threefold degeneracy stems from Landau-type charge order, as revealed by the static charge-structure factor Eq. (2) depicted in Figs. 3(a) and 3(b). For $V_1 > 0$, it peaks at $\pm\mathbf{K}$; the peaks grow when stronger V_1 enhances charge order. As discussed above, this CDW has three quasidegenerate ground states. We thus conclude that we have five FCI states (corresponding to $\nu = 2/5$ or $\nu = 3/5$) for each of the three ground states of the CDW, totaling to the 15 ground states. Five FCI states per CDW state exhibit spectral flow, as seen in Fig. 2, and return to

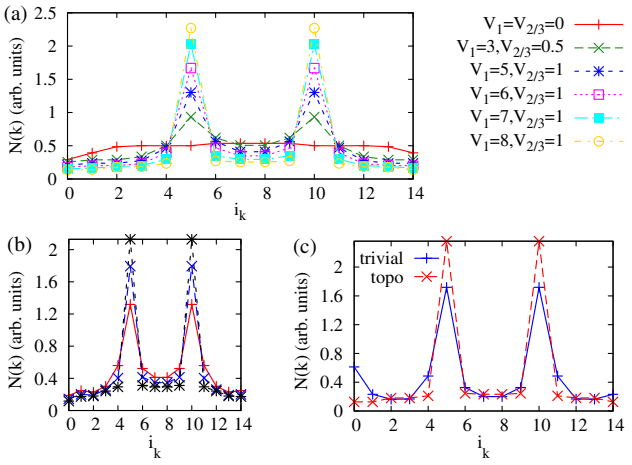

FIG. 3 (color online). Charge-structure factor $N(\mathbf{k})$. (a) $\bar{n} = 12/30$ and (b) $\bar{n} = 13/30$, $V_2 = V_3 = 2t$, and $V_1 = 8t$ (+), $V_1 = 10t$ (×), and $V_1 = 12t$ (*). (c) Comparison of topologically trivial and nontrivial kinetic energy for $V_1/t = 10$, $V_2 = V_3 = 2t$. $t' = 0.2t$ and in the trivial case, $g_3 = m = 2t$ [47]. Of the 15 available momenta, numbers 5 and 10 correspond to the ordering momenta $\pm\mathbf{K}$ of the CDW.

the original point after insertion of five fluxes. The CDW itself does not rely on band topology: Going to a topologically trivial mass term $g_3 = 2t = \text{const}$ [47] somewhat favors a competing sublattice ordering, but charge order nevertheless remains strong; see Fig. 3(c). However, the state is then topologically trivial with $\sigma_H = 0$.

Comparison of the phase diagram Fig. 4 to Fig. 1(a) shows that the TPL needs stronger interactions than the simple CDW at $\bar{n} = 1/3$, consistent with observations in supersolids [36]. In contrast to the pure FCI, the TPL is not induced more easily for the nearly dispersionless bands at $t' \approx 0.2t$ than for more dispersive bands. Moreover, 18 electrons (i.e., 12 holes) also show a TPL with charge order, 15 ground states, and $\sigma_H = -0.4$, even though the "lower" band for holes is quite dispersive [48]. This may be connected to an intrinsically reduced dispersion in the pinball state [40], or it may be due to the rather strong interactions needed to stabilize a CDW, which can then overcome substantial dispersion [25]. Interactions, together with band topology and a partial frustration of the CDW, dominate here over the details of the lower Chern band that were important at weaker interactions. We also note that the illustration of Fig. 1(b) does not fully capture the correlated quantum character of the TPL: for perfect charge order and $t' = 0$, the lowest subband of the effective system is not a Chern band, yet, charge fluctuations at finite V_1 allow a TPL; see Fig. 4.

Nevertheless, we can exploit this picture—valid in the limit of strong V_1—to address larger systems; see the Supplemental Material [48]. We restrict the Hilbert space to low-energy states; i.e., we remove states with too many pairs of particles occupying NN bonds and paying V_1. For $V_1 \gg t$, the CDW becomes perfect and remaining particles

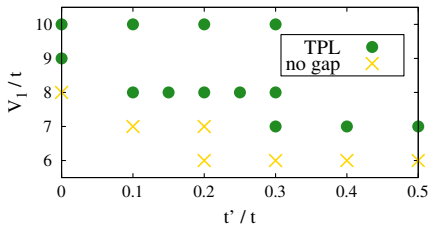

FIG. 4 (color online). Phase diagram for $\bar{n} = 12/30$ depending on V_1 and t' for $V_2 = V_3 = 2t$. Filled circles denote TPL states, × denotes states that do not show a gap between the lowest 15 states and the rest of the spectrum for all fluxes $\boldsymbol{\varphi} = (\varphi_{\mathbf{a}_2}, \varphi_{\mathbf{a}_3})$ [48].

move on the effective honeycomb lattice of Fig. 1(b). Up to six particles moving on a 60-site honeycomb model then become accessible (corresponding to 90 triangular-lattice sites, of which 30 are occupied by the CDW). Indeed, the signatures of the $\nu = 2/5$ FCI component are found, as is expected for a TPL with $\nu = 12/15$.

In conclusion, we have presented numerical evidence for a class of composite states of spinless fermions exhibiting both Landau and topological order. The eigenvalue spectra of our interacting spinless-fermion model on the triangular lattice at filling fractions $\nu = 12/15 = 4/5$ and $13/15$ hint at ground states that are neither FCI nor CDW but have features of both. The Landau order, commensurate charge modulation in the ground states, reveals itself in the interaction-strength-dependent peaks in the static charge-structure factor. The topological order is established via the Hall conductivity, which is precisely quantized, but with a value $\sigma_H \neq \nu$. Instead, we find a quantization consistent with viewing the ground states as composites of a CDW state and a FCI state formed by additional particles in the part of the lattice that remains unoccupied by the CDW, in some sense similar to the superfluid coexisting with a CDW in a supersolid.

These states with coexisting Landau and topological order mix both bands of the model, with Chern numbers $C = \pm 1$, and are made possible by the geometric frustration of the triangular lattice. The TPL is thus a state that arises out of lattice features that go beyond the single-band picture usually sufficient to describe FCIs and definitely goes beyond a Landau-level description. In contrast to FCIs arising in a magnetically ordered system [8,49], where Landau order is found in a different degree of freedom, both types of order are here in the charge sector. In analogy to the supersolid or pinball liquid connection on the triangular lattice, similar states might be found on other lattices supporting supersolids or pinball liquids, possibly also in multiorbital settings [50].

This work was supported by the Emmy-Noether program (Grant No. DA 1235/1-1) of the Deutsche Forschungsgemeinschaft (DFG). We thank A. Ralko, J. Venderbos, I. Vincon, T. Neupert, and P. Kotetes for helpful discussions.

[1] X.-G. Wen and Q. Niu, Phys. Rev. B **41**, 9377 (1990).
[2] T. Neupert, L. Santos, C. Chamon, and C. Mudry, Phys. Rev. Lett. **106**, 236804 (2011).
[3] E. Tang, J.-W. Mei, and X.-G. Wen, Phys. Rev. Lett. **106**, 236802 (2011).
[4] K. Sun, Z. Gu, H. Katsura, and S. Das Sarma, Phys. Rev. Lett. **106**, 236803 (2011).
[5] D. N. Sheng, Z.-C. Gu, K. Sun, and L. Sheng, Nat. Commun. **2**, 389 (2011).
[6] N. Regnault and B. A. Bernevig, Phys. Rev. X **1**, 021014 (2011).
[7] J. W. F. Venderbos, M. Daghofer, and J. van den Brink, Phys. Rev. Lett. **107**, 116401 (2011).
[8] J. W. F. Venderbos, S. Kourtis, J. van den Brink, and M. Daghofer, Phys. Rev. Lett. **108**, 126405 (2012).
[9] X.-L. Qi, Phys. Rev. Lett. **107**, 126803 (2011).
[10] Y.-L. Wu, N. Regnault, and B. A. Bernevig, Phys. Rev. B **86**, 085129 (2012).
[11] C. H. Lee, R. Thomale, and X.-L. Qi, Phys. Rev. B **88**, 035101 (2013).
[12] B. A. Bernevig and N. Regnault, Phys. Rev. B **85**, 075128 (2012).
[13] S. A. Parameswaran, R. Roy, and S. L. Sondhi, Phys. Rev. B **85**, 241308 (2012).
[14] G. Murthy and R. Shankar, Phys. Rev. B **86**, 195146 (2012).
[15] C. Chamon and C. Mudry, Phys. Rev. B **86**, 195125 (2012).
[16] N. R. Cooper and J. Dalibard, Phys. Rev. Lett. **110**, 185301 (2013).
[17] N. Y. Yao, A. V. Gorshkov, C. R. Laumann, A. M. Läuchli, J. Ye, and M. D. Lukin, Phys. Rev. Lett. **110**, 185302 (2013).
[18] D. Xiao, W. Zhu, Y. Ran, N. Nagaosa, and S. Okamoto, Nat. Commun. **2**, 596 (2011).
[19] P. Ghaemi, J. Cayssol, D. N. Sheng, and A. Vishwanath, Phys. Rev. Lett. **108**, 266801 (2012).
[20] Z. Liu, Z.-F. Wang, J.-W. Mei, Y.-S. Wu, and F. Liu, Phys. Rev. Lett. **110**, 106804 (2013).
[21] S. A. Parameswaran, R. Roy, and S. L. Sondhi, arXiv:1302.6606v1.
[22] C. Nayak, A. Stern, M. Freedman, and S. Das Sarma, Rev. Mod. Phys. **80**, 1083 (2008).
[23] A. G. Grushin, T. Neupert, C. Chamon, and C. Mudry, Phys. Rev. B **86**, 205125 (2012).
[24] S. Yang, K. Sun, and S. Das Sarma, Phys. Rev. B **85**, 205124 (2012).
[25] S. Kourtis, J. W. F. Venderbos, and M. Daghofer, Phys. Rev. B **86**, 235118 (2012).
[26] G. S. Kliros and N. d'Ambrumenil, J. Phys. Condens. Matter **3**, 4241 (1991).
[27] A. S. Sørensen, E. Demler, and M. D. Lukin, Phys. Rev. Lett. **94**, 086803 (2005).
[28] Y.-F. Wang, H. Yao, C.-D. Gong, and D. N. Sheng, Phys. Rev. B **86**, 201101 (2012).
[29] M. Trescher and E. J. Bergholtz, Phys. Rev. B **86**, 241111 (2012).
[30] A. Läuchli, Z. Liu, E. J. Bergholtz, and R. Moessner, Phys. Rev. Lett. **111**, 126802 (2013).
[31] C. Hotta and N. Furukawa, Phys. Rev. B **74**, 193107 (2006).
[32] S. Nishimoto, M. Shingai, and Y. Ohta, Phys. Rev. B **78**, 035113 (2008).
[33] L. Cano-Cortés, A. Ralko, C. Février, J. Merino, and S. Fratini, Phys. Rev. B **84**, 155115 (2011).
[34] S. Morohoshi and Y. Fukumoto, J. Phys. Soc. Jpn. **77**, 023708 (2008).
[35] M. Boninsegni and N. Prokof'ev, Phys. Rev. Lett. **95**, 237204 (2005).
[36] S. Wessel and M. Troyer, Phys. Rev. Lett. **95**, 127205 (2005).
[37] R. G. Melko, A. Paramekanti, A. A. Burkov, A. Vishwanath, D. N. Sheng, and L. Balents, Phys. Rev. Lett. **95**, 127207 (2005).
[38] D. Heidarian and K. Damle, Phys. Rev. Lett. **95**, 127206 (2005).
[39] M. Boninsegni and N. V. Prokof'ev, Rev. Mod. Phys. **84**, 759 (2012).
[40] J. Merino, A. Ralko, and S. Fratini, Phys. Rev. Lett. **111**, 126403 (2013).
[41] I. Martin and C. D. Batista, Phys. Rev. Lett. **101**, 156402 (2008).
[42] Q. Niu, D. J. Thouless, and Y. S. Wu, Phys. Rev. B **31**, 3372 (1985).
[43] D. Xiao, M. C. Chang, and Q. Niu, Rev. Mod. Phys. **82**, 1959 (2010).
[44] R. Tao and Y. S. Wu, Phys. Rev. B **30**, 1097 (1984).
[45] D. J. Thouless, Phys. Rev. B **40**, 12034 (1989).
[46] A. Kol and N. Read, Phys. Rev. B **48**, 8890 (1993).
[47] Additionally, the third-neighbor hopping along $\mathbf{a}_3$ only was set to 0; the lower band then has a similarly flat dispersion as in the topological case.
[48] See Supplemental Material at http://link.aps.org/supplemental/10.1103/PhysRevLett.113.216404 for additional data on the stability range of the TPL.
[49] T. Neupert, L. Santos, S. Ryu, C. Chamon, and C. Mudry, Phys. Rev. B **84**, 165107 (2011).
[50] F. Trousselet, A. Ralko, and A. M. Oleś, Phys. Rev. B **86**, 014432 (2012).